Published in final edited form as:
Dev Biol. 2012 January 15; 361(2): 326–337. doi:10.1016/j.ydbio.2011.10.028.

Cell autonomy of DSCAM function in retinal development

Peter G. Fuerst[1,3], **Freyja Bruce**[2], **Ryan P. Rounds**[1], **Lynda Erskine**[2], and **Robert W. Burgess**[3]

[1]Department of Biological Sciences and WWAMI Medical Education Program, University of Idaho, Moscow, ID 83844, USA

[2]The University of Aberdeen, Aberdeen, UK

[3]The Jackson Laboratory, Bar Harbor, ME 04609, USA

Abstract

Cell adhesion molecules (CAMs) provide identifying cues by which neural architecture is sculpted. The Down Syndrome Cell Adhesion Molecule (DSCAM) is required for many neurodevelopmental processes in different species and also has several potential mechanisms of activity, including homophilic adhesion, homophilic repulsion and heterophilic interactions. In the mouse retina, *Dscam* is expressed in many, but not all neuronal subtypes. Mutations in *Dscam* cause the fasciculation of dendrites of neighboring homotypic neurons, indicating a role in self-avoidance among cells of a given type, a disruption of the non-random patterning of their cell bodies, and a decrease in developmental cell death in affected cell populations. In order to address how DSCAM facilitates retinal pattering, we developed a conditional allele of *Dscam* to use alongside existing *Dscam* mutant mouse strains. Conditional deletion of *Dscam* reproduces cell spacing, cell number and dendrite arborization defects. Inducible deletion of *Dscam* and retinal ganglion cell depletion in *Brn3b* mutant retinas both indicate that these DSCAM-mediated phenotypes can occur independently. In chimeric retinas, in which wild type and *Dscam* mutant cells are comingled, *Dscam* mutant cells entangle adjacent wild type cells of the same type, as if both cells were lacking *Dscam*, consistent with DSCAM-dependent cell spacing and neurite arborization being mediated through homophilic binding cell-to-cell. Deletion of *Dscam* in specific cell types causes cell-type-autonomous cell body spacing defects, indicating that DSCAM mediates arborization and spacing by acting within given cell types. We also examine the cell autonomy of DSCAM in laminar stratification and find that laminar disorganization can be caused in a non-cell autonomous fashion. Finally, we find *Dscam* dosage-dependent defects in developmental cell death and amacrine cell spacing, relevant to the increased cell death and other disorders observed in Down syndrome mouse models and human patients, in which *Dscam* is present in three copies.

Introduction

The neural retina offers an ideal system in which to determine how genes mediate the organization of neurons into functional circuits. The retina is organized in both radial and

For Correspondence: Peter G. Fuerst, Department of Biological Sciences, 239 Gibb Hall, University of Idaho, Moscow, ID 83844, Fuerst@uidaho.edu.

circumferential space (vertical and horizontal planes in whole mount preparations). Vertically, the retina consists of three nuclear layers, containing the cell bodies of neurons, separated by two synaptic layers, which contain the chemical synapses and gap junctions that connect the estimated fifty-five basic types of retinal neurons into the functional circuitry of visual detection (Masland, 2001). Both the nuclear and synaptic layers can be further subdivided into different laminae that contain the cell bodies or processes of specific neuronal subtypes. Retinal neurons are also organized in the horizontal plane of the retina. Different aspects of visual processing are performed by different retinal circuits, many of which are spaced in a roughly even manner within the retinal nuclear layers, in patterns called mosaics (Wassle and Riemann, 1978). This organization is thought to ensure that different regions of the retina will contain representation from all of the various circuits by which different aspects of vision, such as motion detection or color discrimination, are detected (Sanes and Zipursky, 2010).

In vertebrates, the Down Syndrome Cell Adhesion Molecule (DSCAM) is required for regulation of cell number, neurite arborization, lamination and segregation of ipsilateral projections in the lateral geniculate nucleus (Blank et al., 2011; Fuerst et al., 2009; Fuerst et al., 2008; Yamagata and Sanes, 2008). In the absence of *Dscam*, cells within the mouse retina that would normally express the gene are not organized in evenly spaced horizontal mosaics, but are arranged in cell type specific clumps, knotted together by densely fasciculated neurites (Fuerst et al., 2009; Fuerst et al., 2008). In the chick retina, DSCAMs, and the closely related Sidekick cell adhesion molecules, are required for the laminar specificity of dendrite arborization in the plexiform layers (Yamagata and Sanes, 2008). In addition to functioning in self-avoidance, vertebrate DSCAMs can also bind the heterologous ligands netrin and draxin and function in axon guidance (Ahmed et al., 2011; Liu et al., 2009; Ly et al., 2008).

Studies of Drosophila have established that DSCAM1-mediated self-avoidance and repulsion occur through isoform-specific homophilic binding (Schmucker et al., 2000; Wojtowicz et al., 2007). Drosophila *Dscam1* undergoes extensive alternative splicing, resulting in isoform diversity that allows the protein to mediate avoidance between the dendrites or axon branches of individual neurons, each of which expresses a different complement of *Dscam1* isoforms and is thus uniquely identified (Hattori et al., 2007; Hughes et al., 2007; Wang et al., 2002; Zhan et al., 2004; Zhu et al., 2006). Because each individual neuron expresses a different subset of *Dscam1* isoforms, different neurons are able to overlap and *Dscam* is able to specify repulsion of axon or dendrite branches in each individual cell (isoneuronally). The molecular diversity of *Dscam1* is essential for its normal function in Drosophila (Hattori et al., 2007; Hughes et al., 2007; Matthews et al., 2007; Soba et al., 2007). Unlike Drosophila *Dscam1*, vertebrate *Dscams* are not subject to extensive alternative splicing and the neurites of *Dscam*-expressing cell types overlap to a considerable degree, even within a single cell type, complicating a repulsive mechanism (Keeley and Reese, 2010). Surprisingly, despite the reduced molecular complexity of vertebrate *Dscams*, the vertebrate gene seems to mediate a similar repulsion or self-avoidance to like neurites, and the loss of *Dscam* results in the clumping and fasciculation phenotypes described.

Here we seek to better understand how vertebrate Dscams achieve this function by testing the cell autonomy of DSCAM activity in retinal development to determine if the protein acts through homophilic or heterophilic binding and by determining if the protein mediates soma spacing and dendrite arborization within a single cell type through self-avoidance or between cell types through adhesion. Results indicate that arborization and spacing are indeed mediated by homophilic DSCAM interactions that act within cell-types to facilitate

self-avoidance, while DSCAM-dependent regulation of laminar specificity can occur in a non-cell autonomous manner.

Results

Dscam is required for a range of developmental processes in the mouse retina. The *Dscam* loss of function phenotype has first been reported at late embryonic stages of development, when retinal ganglion cells in mutant mice begin to develop hyper-fasciculated processes and clumped cell bodies (Fuerst et al., 2009). Fasciculation and clustering of cells that would normally express *Dscam* are observed in a cell-type-specific fashion. For example, a given type of amacrine or ganglion cell will fasciculate with other cells of the same type, but generally not with other cell types (Figure 1A and B) (Fuerst et al., 2009; Fuerst et al., 2008). The affected cell types are also overly abundant, due to a decrease in developmental cell death. Outside of the retina, *Dscam*-deficient retinal ganglion cell axons project through the optic nerve to appropriate CNS targets, but defects in segregation of ipsilateral projections to the lateral geniculate nucleus (LGN) occur in a dose dependent manner (Blank et al., 2011).

Conditional allele of *Dscam*

To better understand whether these functions of Dscam in retinal development depend on homophilic interaction between DSCAMs, whether the phenotypes observed have separate etiologies or stem from a common defect, and whether there is a specific period during development in which *Dscam* is required, a conditional allele of *Dscam* was developed. The *Dscam* conditional allele was generated by flanking exon 27, encoding the *Dscam* transmembrane domain, with loxP sites using standard ES cell homologous recombination (Figure 1C and Supplemental Figure 1 for allele genotyping). The homozygous floxed allele, referred to as $Dscam^{F/F}$, is viable and has no overt neurological phenotypes prior to Cre expression. In the retina, these mice have normal spacing and arborization of retinal dopaminergic amacrine (DA) cells and other assayed neuron types (Figure 1D and E and data not shown). To test if deletion of the transmembrane domain would recapitulate other *Dscam*-mutant alleles, the $Dscam^{F/F}$ mice were bred to transgenic mice expressing Cre recombinase under the control of the *Pax6α* promoter (Marquardt et al., 2001). *Pax6α* Cre is broadly expressed in most types of retinal neurons, except a swath in the central-dorsal retina in which only amacrine cells are targeted (Stacy et al., 2005.). DA cells in the $Dscam^{F/F}$ *Pax6α* Cre retina fasciculate and aggregate, comparable to other *Dscam* mutant strains (Fuerst et al., 2010; Fuerst et al., 2008). This confirms that deletion of the DSCAM transmembrane domain reproduces the *Dscam* spacing and arborization phenotypes seen in other strains of *Dscam*-mutant mice, despite leaving the coding sequence in frame (Figure 1F).

Deletion of the floxed allele was also performed in the germ-line, referred to as $Dscam^{FD}$, to assay the effect of global deletion of the DSCAM transmembrane domain. In addition to phenocopying other *Dscam*-mutant alleles, a dosage dependent phenotype was observed in DA cells. DA cells in wild type and $Dscam^{F/F}$ retina were rarely located in close proximity to other DA cells. The number of DA cells directly abutting other DA cells was counted in $Dscam^{F/F}$ and $Dscam^{FD/F}$ retinas. A significant increase in the number of DA cells abutting other DA cells was observed in $Dscam^{FD/F}$ retinas compared to $Dscam^{F/F}$ retinas (Figure 1G–I). This indicates that a previously reported DSCAM-dosage phenotype observed in melanopsin-positive RGCs (mRGCs) can be generalized across multiple types of neurons (Blank et al., 2011). The extensive fasciculation between $Dscam^{FD/FD}$ DA cells was not observed in $Dscam^{FD/+}$ *or* $Dscam^{FD/F}$ retinas, suggesting that at intermediate *Dscam* dosage regulation of cell spacing is disrupted without disruption of arborization (Figure 1G–I and data not shown).

Independence of fasciculation and cell number phenotypes

An increase in cell number through a decrease in cell death is observed in the *Dscam* mutant retina in conjunction with fasciculation and mispatterning of cell bodies. These phenotypes could all derive from a common defect, for instance, decreased cell death leading to increased cell number and therefore increased interaction between processes, resulting in fasciculation and misplaced cell bodies. However, the observation of DA cell spacing defects in the absence of fasciculation or increased cell number suggested the phenotypes might occur independently of each other (Figure 1H). We therefore tested whether the defects observed in the *Dscam* null retinas are independent of each other, or if a single primary defect can give rise to the other phenotypes secondarily. We reasoned that temporally controlled deletion of *Dscam* could separate phenotypes, and *Dscam* was therefore targeted for deletion at various time points during development. Tamoxifen was given to activate a Cre-estrogen receptor fusion (Esr Cre) in a transgenic mouse strain with the ESR Cre driven ubiquitously by the CAGGS-promoter (Hayashi and McMahon, 2002). Tamoxifen administration at all tested ages resulted in similar widespread activation of the Thy1-Stop-YFP Cre reporter (data not shown) (Campsall et al., 2002). Induction of Cre activity at E13 and E16 reproduced a null phenotype in both DA cells and mRGCs when assayed at postnatal days 0 (mRGCs; P0) and 20 (mRGCs and DA cells; P20) (Figure 2A and B and data not shown). Induction of Cre activity at P0 resulted in 2–3 fasciculated groups of mRGCs in each retina and no apparent change in cell number (Figure 2C, D). In DA cells, induction of Cre activity at P0 resulted in a statistically significant increase (T-Test< 0.05) in DA cell number, but no fasciculation (Figure 2E and G). Density Recovery Profile (DRP) analysis, a measure of how likely a cell of a given type will be located a given distance from another cell of the same type, was performed to determine if deletion of *Dscam* at P0 influenced the spacing of DA cells. DRP analysis is performed by plotting the location of all cells of a given type within a field. The number of cells at a given distance from a given cell, termed the reference soma, is counted for every cell in the field. The number of cells at a given distance from other cells of the same type is plotted on the Y-axis. Distance from the reference soma is plotted in binned distances from the location of the reference soma on the X-axis. If cells are organized so as to avoid proximity to other cells of the same type, then the number of cells located in close proximity to the reference soma will be lower than the average cell density. This dip in cell number in close proximity to the reference soma is termed the exclusion zone. If cells are randomly distributed a number of cells close in value to the average cell density will be found regardless of distance to the reference soma. If cells are clustered, such that they are more likely to be found near other cells of the same type, the number of cells at close proximities to the reference soma will be higher than the average cell density. Both assayed genotypes maintained a DA cell exclusion zone. The exclusion zone appears weaker in the P0 targeted retinas, but this could simply reflect the increased cell density in this genotype (Figure 2F and H). In order to compare the DRP charts of genotypes in which the cell density is changed, the packing index of each genotype was calculated. The packing index is determined by calculating the effective radius, a measure of the distance cells of the same cell type are excluded around an average cell of that type, and the maximum radius, the hypothetical maximum distance cells can be spaced at a given density, as if they are arranged in a hexagonal pattern (Rodieck, 1991). The packing index thus scales independently of density. No significant difference was found when comparing the packing index of DA cells in control and P0 targeted retinas. These data indicate that an increase in cell number often observed in the *Dscam*-deficient retina is not sufficient to give rise to fasciculation or disrupt mosaic spacing. No changes in retinal architecture were detected associated with Cre induced deletion of *Dscam* in the adult retina (data not shown).

We further tested the relationship between *Dscam*-deficient phenotypes by depleting RGC number to assay if fasciculation in the absence of *Dscam* would still occur when cell number is reduced. Retinal ganglion cells were genetically depleted using a *Brn3b*-null mutation (Gan et al., 1996). In the *Brn3b* mutant retina, retinal ganglion cell number is approximately 15% that of wild type. Increased fasciculation is evident in P3 mRGCs in *Dscam*-mutant retinas compared to wild type (Figure 2I and J). As expected, a decrease in RGC cell number was observed in the P3 $Dscam^{+/+}$; $Brn3b^{-/-}$ retina and cells are still spaced from one another and processes are arborized (Figure 2K). In $Dscam^{FD/FD}$;$Brn3b^{-/-}$ retinas, the mRGCs that remain were bound in dense aggregates resulting in pockets of mRGCs separated by large sections of retina devoid of mRGCs (Figure 2L and Supplemental Figure 2). This indicates that fasciculation and cell number increases observed in the *Dscam*-deficient retina can occur independently of each other.

DSCAM regulates cell death in a dose dependent fashion

The spacing and fasciculation of DA cells and mRGCs are semi-dominant phenotypes that are sensitive to *Dscam* gene dosage (Blank et al., 2011; Fuerst et al., 2008). To determine if developmental cell death was also sensitive to DSCAM dosage, cleaved caspase3 (CC3) positive neurons were assayed in developing retinas from wild type, $Dscam^{del17/del17}$ and $Dscam^{del17/+}$ mice. Deletion of *Dscam* results in a dramatic decrease in retinal developmental cell death at postnatal days 0 (P0), P3 and P5 (Figure 2M). The decrease in cell death was dose dependent with $Dscam^{+/del17}$ heterozygous retinas having a level of cell death roughly intermediate to that observed in wild type and $Dscam^{del17/del17}$ homozygous retinas. Therefore, while cell number, spacing and neurite fasciculation are not causally related, they are all similarly sensitive to *Dscam* dosage.

DSCAM functions with cell-type autonomy

DSCAM has multiple potential mechanisms by which it could mediate neurodevelopment. DSCAM can bind the heterologous ligand netrin or act as a homophilic cell adhesion molecule, through which it may mediate both adhesion and repulsion (Agarwala et al., 2000; Andrews et al., 2008; Fuerst et al., 2009; Liu et al., 2009; Ly et al., 2008; Yamagata and Sanes, 2008). Most models of Dscam's activity in retinal development presuppose that it operates through homophilic recognition, resulting in cell autonomous phenotypes (Fuerst and Burgess, 2009; Sanes and Zipursky, 2010). We therefore sought to determine if fasciculation, spacing and lamination do indeed depend on cell-cell homophilic interaction.

In the wild type vertebrate retina, many neurons of a given type are spaced in a non-random mosaic pattern, often with overlapping dendrites (as diagrammed in Figure 3A). In the *Dscam*-deficient retina, cells that would normally express *Dscam* have fasciculated dendrites and aggregated cell bodies (Figure 3B). The conditional *Dscam* allele was used to generate chimeric retinas, in which wild type and mutant neurons were commingled. If DSCAM acts as a receptor for a heterologous ligand, or acts primarily within single neurons, wild type cells in a chimeric retina would be predicted to maintain their normal patterning, whereas mutant cells would be predicted to have a mutant phenotype (Figure 3C). Conversely, if DSCAM activity is mediated through homophilic DSCAM-DSCAM interactions between cells, its expression would be required in both interacting cells, and therefore in chimeric retinas, mutant cells should entangle and adhere to adjacent wild type cells as if both cells lacked *Dscam* (Figure 3D).

Chimeric retinas were generated using cre expression under the control of the *Chx10* promoter, which is expressed in a subset of clonal columns at approximately embryonic day 10.5 (Rowan and Cepko, 2004). A dual Cre reporter integrated in the *Rosa* locus was used to label portions of the retina in which Cre is active. In this strain, a dsRED reporter is

expressed in all tissues until Cre activity, after which dsRED and a stop cassette upstream an eYFP gene are deleted, converting the cell from dsRED-positive to eYFP-positive (Muzumdar et al., 2007). Aggregation of wild type (red) with *Dscam*$^{del17/del17}$ (green) DA cells is observed in *Chx10* Cre derived chimeric retinas (Figure 3E). Targeting *Dscam* with Pax6*α* Cre resulted in a similar phenotype, in which wild type and mutant or multiple mutant cells would aggregate (Figure 3F).

Similar results were obtained in RGCs, most of which express *Dscam* (Fuerst et al., 2009). Both melanopsin-positive RGCs (mRGCs) and alpha RGCs, labeled with the Smi-32 antibody, had fasciculated dendrites and formed homotypic clumps in the *Dscam*$^{del17/del17}$ retina (Fuerst et al., 2009). To examine the cell autonomy of DSCAM function in retinal ganglion cells (RGCs), we generated chimeric mice using *cre* under control of the *Thy1.2* promoter to delete *Dscam* from a subset of RGCs (Campsall et al., 2002). In chimeric *Dscam*$^{F/F}$ *Thy1.2* Cre retinas, wild type mRGCs and alpha-RGCs did not fasciculate and aggregate with other wild type cells, but did aggregate with mutant cells of the same type (Figure 3G and H). Therefore, in both amacrine and ganglion cells, DSCAM functions homophilically cell-to-cell.

Antibodies with suitable specificity were not available to reliably confirm *Dscam* deletion in targeted cells labeled as Cre-positive by the reporters. We therefore used a second approach to independently confirm that DSCAM acts homophilically and also to test if the *Dscam*^{del17} allele, with an internal deletion/frame shift mutation in exon 17, would result in a similar phenotype. Chimeric retinas were generated by injecting GFP transgenic ES cells (wild type for *Dscam*) into *Dscam*$^{del17/del17}$ blastocysts (Figure 3I). Wild type and *Dscam*$^{del17/del17}$ dopaminergic amacrine (DA) cells were found in chimeric retinas, and these were imaged to assess their respective morphologies and patterning. Wild type DA cells (GFP-positive) were found to fasciculate and/or aggregate with *Dscam*$^{del17/del17}$ DA cells (GFP-negative), but were rarely found in close proximity to other wild type cells, similar to the pattern observed in the wild type retina (Figure 3J–K). The neurites of wild type cells, whether located adjacent to mutant DA cells (Figure 3J) or separated from mutant DA cells (Figure 3K and L) were incorporated into fascicules (small red and yellow arrowheads). Forty-two aggregates were composed of mutant cells only, twenty nine aggregates were composed of wild type and mutant cells, and three examples of juxtaposed wild type cells were counted in two retinas in which we assessed a total of 359 mutant cells and 161 wild type cells. Therefore, in both RGCs and amacrine cells, *Dscam* facilitates spacing and arborization in a cell type autonomous manner, by which we mean that expression is required in all cells of a given type, consistent with a requirement for homophilic DSCAM-DSCAM interaction cell to cell.

Cell types respond independently to *Dscam* deletion

Cre lines that delete in specific cell types were used to further test the cell autonomy of *Dscam* and to establish that phenotypes in postsynaptic ganglion cells were not due to mispatterning of presynaptic amacrine cells, or vice versa. *Dscam* was targeted for deletion with transgenic Cre recombinase lines that are active in either retinal ganglion cells, amacrine cells or a mixture of both. *Dscam* was targeted in a large population of retinal ganglion cells using *Brn3b* driven Cre, or in mRGCs using an *Opn4* driven Cre (*Opsin4*; the melanopsin gene promoter). *Dscam* was targeted in amacrine cells using *Ptf1A* Cre, which is expressed in GABAergic amacrine cells, *TH* Cre, which is expressed in dopaminergic amacrine cells, or Pax6 α Cre (Kawaguchi et al., 2002; Savitt et al., 2005). Cre lines were found to be active in the expected cell types with minimal activity in off target cell populations (Supplemental Figure 3). The *Opn4* Cre line targeted many types of RGCs, likely reflecting the broad expression of melanopsin in developing RGCs (Ecker et al.,

2010). One of two TH Cre lines produced a variable spacing defect in DA cells, but this result was inconsistent, possibly as a result of the fluctuating number of DA cells targeted by this Cre line (Supplemental Figure 3K and Supplemental Figure 4). A second TH-Cre line did not express in DA cells (Table 1).

Cell body spacing was assessed in amacrine cells using DRP analysis following deletion of *Dscam* in GABAergic amacrine cells using *Ptf1A*-driven Cre (Figure 4A–D). Spacing and arborization of type I bNOS-positive amacrine cells in the inner nuclear layer, which require DSCAM for normal mosaic spacing and arborization, were disrupted as a result of *Dscam* deletion in GABAergic amacrine cells, although the large increase in cell number observed in the $Dscam^{del17/del17}$ retina was not observed (Fuerst et al., 2008). A statistically significant change in the packing index (T-Test=0.027) indicated that targeting *Dscam* in GABAergic amacrine cells disrupts the spacing of this population of bNOS-positive amacrine cells. Deletion of *Dscam* in RGCs using *Brn3b* Cre caused a fasciculation and spacing phenotype in melanopsin-positive and alpha RGCs (Figure 4E and F and Supplemental Figure 3). Deletion of *Dscam* in melanopsin-positive RGCs using *Opn4* Cre caused a fasciculation and aggregation phenotype in these cells (Figure 4G–H). Therefore, deletion of *Dscam* in a specific cell class reproduces to varying degrees the *Dscam*-mutant phenotype in at least the targeted cell type. The failure to completely recreate the *Dscam* null phenotype in amacrine cells may be a function of when the cre is activated, the number of cells in which *Dscam* is deleted, or may indicate some additional disorganization arising through interactions between other cell types when the entire retina is deleted for *Dscam* and not just a specific cell type.

Dscam does not facilitate mosaic patterning or arborization by acting between tested cell types

DSCAM has been shown to act in organization of the retina in both the horizontal and vertical planes (Fuerst et al., 2009; Yamagata and Sanes, 2008). Deletion of *Dscam* results in a cell autonomous mutant phenotype within a cell type, and wild type cells of a given cell type will adopt a mutant phenotype when integrated into a retina containing other mutant cells (Figures 3–4). To test if DSCAM mediates arborization and spacing within, or between, cell types, *Dscam* was targeted for deletion in either amacrine or retinal ganglion cells after which the presence of a mutant phenotype was assayed in the wild type synaptic partners of the deleted cell type.

For this, we first took advantage of the chimeric retinas generated with *Pax6α* Cre, which is expressed in retinal neurons throughout the peripheral and ventral retina but only in amacrine cells in a stripe running dorsal to ventral through the center of the retina. *Pax6α* Cre activity in amacrine cells in the inner nuclear layer (INL) is sufficient to disorganize DA cells, even in portions of the INL that are overlaid by portions of the retinal ganglion layer (RGL) where *Pax6α* Cre is not active. To more specifically test if *Dscam* deletion and subsequent disorganization of DA cells influences the wild type mRGC synaptic partners of DA cells, we immuno-labeled both cell types in $Dscam^{F/F}$ *Pax6α* Cre retinas (Zhang et al., 2008). DA cells were aggregated in clumps and had fasciculated neurites in both the peripheral retina (Cre-positive), and in the central and dorsal retina (cre-positive only in the INL) (Figure 5A). In contrast, Melanopsin-positive RGCs were fasciculated and aggregated in the peripheral retina, but not in the central or dorsal retina, indicating that disorganization of DA cells is not sufficient to disorganize the arborization or spacing of wild type mRGCs (Figure 5B and Supplemental Figure 5).

As an additional test of whether *Dscam* acts between cell types, deletion of *Dscam* was targeted in retinal ganglion cells using *Brn3b* Cre after which the spacing of DA and bNOS amacrine cells was assayed by density recovery profiling. No significant difference in cell

density or the packing index of either amacrine cell type compared to control was detected, indicating that both of these amacrine cell types maintain mosaic spacing in retinas in which *Dscam* is targeted with *Brn3b* Cre (Figure 5C–J).

Dscam was also targeted for deletion in amacrine cells using *Ptf1a* Cre or *TH* Cre, after which the spacing of retinal ganglion cells was assayed. No obvious fasciculation or difference in the spacing or number of smi32- or melanopsin-positive retinal ganglion cells was observed (Supplemental Figure 6).

Non-autonomous function of DSCAM in laminar specificity

Dscam is not required for laminar stratification of several cell types in which it is expressed despite being required for mosaic spacing and arborization, including DA cells and mRGCs, which instead use semaphorins and plexins to restrict laminar specificity (Fuerst et al., 2009; Matsuoka et al., 2011). Other cell types, including bNOS and cholinergic amacrine cells, have synaptic lamination defects in the $Dscam^{2J/2J}$ allele, a spontaneous frame shift mutation in exon 18 that arose in a C3H genetic background (Fuerst et al., 2010). This finding is consistent with the *Dscam* phenotype observed in the chick retina (Fuerst et al., 2010; Yamagata and Sanes, 2008). The lamination of bipolar, amacrine and retinal ganglion cell populations was assayed in the inner plexiform layer of wild type, $Dscam^{FD/FD}$, $Dscam^{2J/2J}$ and $Dscam^{F/F}$ mice targeted with Pax6α Cre or Brn3b Cre to examine the cell autonomy of lamination defects observed in the *Dscam* mutant retina.

Laminar specificity of several assayed cell types, including DA cells and mRGCs, was not noticeably different when comparing wild type and mutant genotypes, despite the extensive fasciculation observed in mutant retinas, for example the large fascicle of mRGCs present in the $Dscam^{F/F}$ Brn3b Cre retina image (Figure 6A; DA cells and mRGCs and data not shown). Normal lamination in other cell types, described below, is affected by the loss of *Dscam*.

bNOS positive amacrine cells have lamination defects in $Dscam^{2J/2J}$ mutant retinas, and also require DSCAM for normal spacing and arborization (Fuerst et al., 2008). Lamination and fasciculation of bNOS-positive amacrine cells were assayed in wild type, $Dscam^{2J/2J}$, $Dscam^{FD/FD}$ and $Dscam^{F/F}$ Pax6α Cre and Brn3b Cre retinas. Fasciculation was observed in $Dscam^{FD/FD}$, $Dscam^{2J/2J}$ and $Dscam^{F/F}$ Pax6α Cre retinas (Figure 6C and F; arrows and data not shown). Lamination was not disrupted in regions of the Pax6α Cre retina where only amacrine cells were targeted by Cre, even though fasciculation of bNOS positive amacrine cell neurites was observed, and bNOS-amacrine cell neurite lamination was disrupted in regions of the same retina in which Pax6α Cre was more broadly active (Figure 6F and data not shown). Therefore it appears fasciculation of bNOS amacrine cells is the result of cell type specific requirements for *Dscam*, while bNOS-positive lamination defects require the disorganization of non-amacrine cell types.

Dscam expression has not been observed in mouse or chick cholinergic amacrine cells, but these cells do have disrupted lamination in some *Dscam* mutant backgrounds, suggesting the defects observed may be secondary to disorganization of other cell types, or involve heterologous interactions between DSCAM and a non-homophilic ligand (Fuerst et al., 2008; Yamagata and Sanes, 2008, 2010). Variable defects in cholinergic amacrine cell neurite lamination were observed in the $Dscam^{2J/2J}$, $Dscam^{FD/FD}$ and $Dscam^{F/F}$ Brn3b Cre retinas (Figure 6C–K). Cholinergic lamination was impaired in portions of the $Dscam^{F/F}$ Pax6α Cre in which Cre was active in all retinal neurons, but not in portions of the $Dscam^{F/F}$ Pax6α Cre retina in which only amacrine cells, including cholinergic amacrine cells, were targeted (Figure 6F and K and data not shown). Whole wild type and $Dscam^{2J/2J}$ retinas imaged for ChAT show that the laminar discontinuity of cholinergic bands seen in

retinal sections is the result of wide gaps within the uniform cholinergic arbor observed in the wild type retina, consistent with the heavy fasciculation observed in other cell types (Figure 6L and M; Figure 6A; $Dscam^{F/F}$ Brn3b Cre for example of heavy fasciculation). Cholinergic lamination was not disrupted in the $Dscam^{F/F}$ ChAT Cre retina, consistent with cholinergic cells not expressing *Dscam* and further suggesting disruption of their lamination is occurring in a non-cell autonomous manner (data not shown) (Pecho-Vrieseling et al., 2009).

Phenotypes of Cre-mediated deletion of $Dscam^{F/F}$ presented throughout the rest of the manuscript are summarized in Table 1.

Discussion

In this study, we have demonstrated four important features of DSCAM function in mammals. First, we demonstrate that the DSCAM-mediated regulation of dendrite self-avoidance, cell body spacing, and developmental cell death can be independent phenotypes and are not causally related to one another. This was shown using cell-type-specific- and temporally controlled deletion of *Dscam*, which also showed that *Dscam* is required during embryonic and early postnatal ages, but its loss later does not result in a reversal or perturbation of dendritic morphology or mosaic cell body spacing once these properties are established in the mouse retina. Second, analyses of chimeric mice generated through either cell aggregation or incomplete cre-mediated excision of a conditional allele indicate that DSCAM functions in a homophilic manner in self-avoidance. Furthermore, this function is required within cell types, but does not extend between synaptically coupled cell types, an effect we term a cell-type autonomous function. Third, we find that DSCAM regulates cell death in a gene dosage dependent manner and identify a dosage dependent role of DSCAM in spacing of DA cells. Finally DSCAM is required for laminar targeting of some cell types in a non-cell autonomous manner.

Mouse DSCAM has several potential mechanisms by which it could mediate spacing and arborization, for example through either homophilic or heterophilic binding. In *Drosophila*, self-avoidance functions such as dendrite arborization and axon branching are the result of homophilic DSCAM interactions, and these functions occur at the level of individual cells. The extensive alternative splicing of the fly *Dscam1* gene gives each cell its own complement of *Dscam* isoforms. In vertebrates, this molecular diversity is lacking for *Dscams*, so other co-receptors or non-homophilic mechanisms could be involved to increase the specificity and diversity required for self-recognition. Furthermore, other functions of DSCAMs in vertebrates differ from the self-avoidance and adhesion seen in the mouse and chick retinas. These include axon guidance, where DSCAM serves as a receptor for netrin signaling (Li et al., 2009; Liu et al., 2009; Yamagata and Sanes, 2008). The diversity of DSCAM-mediated functions demonstrates that DSCAM can signal through a variety of mechanisms and it was therefore important to determine if the self-avoidance function of DSCAM in the mouse retina requires homophilic interaction.

This does appear to be the case for neurite arborization and spacing. If a mutant cell lacking *Dscam* encounters a wild type cell, the outcome is as if both cells are mutant, consistent with a requirement for DSCAM on both membranes and homophilic recognition. Whereas the deletion of *Dscam* from one cell of a given type can cause a mutant phenotype in other homotypic cells, deletion of *Dscam* from one cell type has ramifications only for that cell type, and effects on other populations are restricted to secondary events caused by neurites being redirected to aberrantly patterned targets (the deleted cell type). Therefore, the mutation does not display perfect cell autonomy, since wild type cells can show a mutant phenotype, but instead shows “Cell-type-autonomy.”

The timing of DSCAM's requirement for self-avoidance is interesting and also implies multiple functions for the protein. *Dscam* has a very dynamic expression pattern and its subcellular localization can also change, redistributing the protein from processes to cell bodies for example (Barlow et al., 2002). DSCAM's role in self-avoidance appears to be restricted to the ages at which neurons are extending processes and thereby encountering the distal processes of neighboring homotypic cells. Deletion of the gene later in development does not result in the same fasciculation and spacing defects observed in constitutively null retinas, or with embryonic or early postnatal induced deletion. Since *Dscam* expression persists into adulthood, it may be serving other roles later. For instance, in the chick, Dscams and related Sidekick proteins bind multi-PDZ domain proteins including PSD95 and the MAGIs, well-established synaptic scaffolding proteins (Yamagata and Sanes, 2010). Indeed, in mouse, DSCAML1 (for which better antisera are available) is localized adjacent to synaptic proteins in the outer plexiform layer of the adult mouse (Fuerst et al., 2009). Perhaps after functioning as anti-adhesive signals early in development, DSCAMs function in the maturation or maintenance of synapses in the adult. Consistent with this, the bipolar cell-rod synapses in mice lacking DSCAML1 were reduced in number and the bipolar-AII amacrine cell synapses had many anatomical and functional characteristics of immature synapses (Fuerst et al., 2009).

The independence of *Dscam* deficiency phenotypes is also important for interpreting mechanisms. For example, it was a formal possibility that the increased cell density caused by decreased cell death in *Dscam* mutant retinas led to increased fasciculation of dendrites and subsequently to mispositioning of cell bodies. For some cell types, the changes in cell density may contribute to the dendrite fasciculation and cell body clumping phenotypes, and our own results (Fuerst et al., 2008) indicate that some cell types transition from being spaced to being clumped as their dendrites become increasingly intertwined. However, the conditional deletion of *Dscam* and other genetic manipulations such as *Brn3b* mutations have allowed us to separate these phenotypes and demonstrate that each is a primary, independent function of DSCAM. For example, deletion of *Dscam* from dopaminergic amacrine cells using temporally controlled, tamoxifen inducible cre increases cell density and randomizes soma spacing, but does not result in fasciculation. The randomization of spacing seen with increased cell density may reflect a failure to sculpt a non-random mosaic pattern through cell death, so some level of interdependency of the phenotypes may exist. However, the extensive clumping of cell bodies seen in the absence of DSCAM, even with the dramatic reduction in RGC density seen with *Brn3b* mutant backgrounds, indicates that the clumping is not entirely secondary to increased cell density nor are changes in the mosaic patterning of cell bodies just a failure to eliminate misplaced cells through apoptosis during development. Similarly, the increased density seen without fasciculation indicates that the lack of cell death is not dependent on survival cues resulting from fasciculation.

Non-autonomous DSCAM-dependent phenotypes were also observed. Some lamination defects are non cell autonomous and likely reflect disorganization of other retinal cells, adhesive interactions that are lost in the absence of DSCAM, or possibly heterologous interactions between DSCAM and another ligand. We have observed apparent switches in synaptic specificity consistent with an adhesive role for DSCAM in some *Dscam* mutant backgrounds but need to confirm that these changes do not simply reflect changes in expression of the antigen markers used to label respective cell types (data not shown). These results are consistent with observations in the chick retina in which both gain and loss of function manipulations of Dscam resulted in changes in laminar specificity (Yamagata and Sanes, 2008). It is also similar to the mistargeting of synaptic partners when on cell type was mislocalized in response to changes in semaphorin signaling (Matsuoka et al., 2011). Finally, the genetic background of mice also seems to influence this phenotype, given that both $Dscam^{del17}$ and $Dscam^{2J}$ alleles are similar frameshift mutations (in exons 17 and 18

respectively), but are on different genetic backgrounds (BALB/c and C3H respectively) and have a differing severity in their laminar specificity phenotypes. Initial results suggest that crossing the *Dscam*^{del17} mutation onto a C3H background results in mice with more disrupted cholinergic and bNOS cell lamination, suggesting that selecting for *Dscam*$^{del17/del17}$ mice that would survive and breed on a mixed C57Bl/6J/Balb/cJ background resulted in reduced overt and retinal phenotypes (data not shown). Therefore, the relative contribution of each of these mechanisms, disorganization, loss of adhesion, loss of a heterophilic interactions, and effects of genetic background, to the non-cell autonomous effects on laminar specificity will need to be further examined.

The use of Dscam by multiple overlapping cell types to facilitate the same function suggests DSCAM acts as part of a larger adhesion code, which is an area of active investigation. The MAGI scaffolding proteins, which bind DSCAMs, have six PDZ docking sites, allowing for a wide range of receptor complexes (Yamagata and Sanes, 2010). We hypothesize that in the absence of DSCAM, MAGI complexes that would otherwise contain DSCAM take on different functions based on the residual docked proteins. These functions may vary between cell types. For example, DSCAM is required in a cell-type-autonomous manner for DA and mRGC spacing and arborization, but not lamination, whereas DSCAM is required in a non-cell autonomous manner for the lamination, but not spacing, of cholinergic amacrine cells. Differences in how diverse retinal cell types use DSCAMs and the markers used in previous studies of DSCAM function are likely to explain the different phenotypes, in repulsion and adhesion, initially observed and attributed to DSCAMs in mouse and chick (Fuerst et al., 2008; Yamagata and Sanes, 2008). A better understanding of how DSCAMs mediate different processes in diverse cell types will require the identification of the combinations of PDZ-interacting proteins that can bind MAGI proteins in combination with Dscam, along with identifying the proteins by which dendrites are adhered to each other in the absence of DSCAM.

The role of *Dscams* in mammalian neurodevelopment is an emerging story. The results of this study demonstrate important aspects of the molecular, temporal, and cellular basis for DSCAM's function in self-avoidance in the mouse retina. Dosage sensitive *Dscam* phenotypes, including cell death, lamination and spacing, are also described. *Dscam* is located in the Down Syndrome critical region and its dosage is increased in Down Syndrome mouse models (Gitton et al., 2002). Down Syndrome mouse models have an increase in neural cell death whereas *Dscam* mutant mice, in which *Dscam* is deficient, have a decrease in retinal cell death (Fuerst et al., 2008; Holtzman et al., 1996). Future studies on these developmental processes are now required to understand the key features of molecular recognition and cell adhesion molecules in neuronal circuit formation and to determine if *Dscam* dosage contributes to human Down syndrome phenotypes.

Materials and Methods

Mouse strains and cell lines

The following mouse strains and cell lines were used in this study: *Dscam*^{del17}: B6.CBy-(*Dscam*^{del17})/RwbJ (Jax stock number 008000) (Fuerst et al., 2008), C3H/HeDiSn-*Dscam*^{2J}/GrsrJ (Jax stock number 006038) (Fuerst et al., 2010), Pax6α Cre: Tg$^{(Pax6\ Cre,GFP)}$/2Pgr, courtesy of Dr. Peter Gruss, (Marquardt et al., 2001; Stacy et al., 2005), Esr Cre: B6.Cg-$^{Tg(CAG\ Cre/Esr1*)/}$5AmcJ (Jax stock number 004682) (Hayashi and McMahon, 2002), Thy1.2 Cre: FVB/N-$^{Tg(Thy1\ Cre)1}$/VlnJ (Jax stock 006143) (Campsall et al., 2002), 7AC5 ES cells (Nagy et al., 1990), Thy1-floxed-stop-YFP reporter strain: Tg$^{(Thy1\text{-}EYFP)15}$/Jrs (Buffelli et al., 2003; Livet et al., 2007), TH Cre: B6.Cg-$^{Tg(Th\ Cre)}$ Tmd/J (Jax stock number 008601) (Savitt et al., 2005), Ptf1A Cre: Ptf1$^{atm1.1(cre)}$/Cvw (MMRRC stock number 000435-UNC), DSRED/YFP reporter strain: B6.129-$^{Gt(ROSA)26Sortm3(CAG\text{-}EGFP/Dsred2)}$Luo/J (Jax stock

number 006075) (Muzumdar et al., 2007), *Opn4* Cre (courtesy of Dr. Samar Hatter) and *Brn3b* Cre (Courtesy of Dr. Vann Bennett).

Animal care and handling

Mice were used in accordance with protocols approved by the Animal Care and Use Committees at The Jackson Laboratory and the University of Idaho. The Jackson Laboratory is accredited by AAALAC. Animals were housed in PIV caging and given food and water ad libitum, and maintained on a 14 hour:10 hour light:dark cycle.

Immunohistochemistry

Enucleated eyes were fixed in 4% paraformaldehyde overnight. Tissue was sunk in 30% sucrose/PBS and frozen in OCT media. 8 μm sections were cut using a cryostat and used immediately or stored up to two weeks at −20° C. Sections were blocked in 3% normal horse serum in 1x PBS and 0.1% triton. Primary antibodies were incubated overnight at 4°C and subsequently washed 2 times for ten minutes in PBS. Sections were incubated at room temperature with secondary antibodies for one hour, and then washed four times in PBS for ten minutes. The last wash contained 2 μl of 1mg/ml Dapi per 40 ml PBS. Sections were cover slipped with an antifade media and stored at 4° C until imaging.

Whole retina staining

Mice were transcardially perfused with PBS and 4% paraformaldehyde. Eyes were enucleated was placed in a dish containing PBS. A small hole was made at the junction between the cilliary body and retina with a 30 gauge needle. The eye was hemisected and the retina was gently teased away from the sclera. Retinas were fixed a second time in 4% paraformaldehyde overnight, followed by a rinse in PBS. Retinas were incubated with primary antibodies in PBS, supplemented with 3% normal horse serum and 0.5% triton-x 100, for 3–5 days at 4° C, with gently rocking. Primary antibodies were washed off overnight in PBS and the retinas were incubated with secondary antibodies in PBS, 3% normal horse serum and 0.5 % triton. Retinas were washed for 2–4 hours in PBS and flat mounted in an antifade media. All fluorescent images were acquired on a Leica SP5 confocal microscope.

Antibodies

The following antibodies were used in this study: SMI-32 mouse anti-non-phosphorylated neurofilament (Covance, SMI-32R at 1:500), Rabbit anti-melanopsin (Generously provided by Ignacio Provencio at 1:10,000), mouse anti-tyrosine hydroxylase (Novocastra, NCL-TH at 1:25), rabbit anti-tyrosine hydroxylase (Millipore, AB152 at 1:500), mouse anti-neurofilament (Developmental Studies Hybridoma Bank, 2H3 at 1:50), goat anti-BRN3b (Santa Cruz Biotechnology, 6026 at 1:400) and mouse anti-PKCα (Santa Cruz Biotechnology, 1:500).

DRP analysis

DRP analysis was performed as previously described (Rockhill et al., 2000; Rodieck, 1991). In these experiments the program winDRP was used compute DRP charts. For DA cells the cell diameter was set at 15 μm, and fifteen annuli, each of 15 μm were used. For type I bNOS amacrine cells the cell diameter was set at 15 μm and twenty annuli of 15 μm each were used. The first annulus was discarded to account for the soma itself and the edge correction option was used to correct for cells located at the margins of the imaged field. Type I bNOS cells were distinguished from type II bNOS cells by their larger soma size and brighter immunoreactivity. The packing index was determined by taking the square of the

quotient of the effective radius and maximum radius $(R_e/R_m)^2$, to test effects on cell body spacing that scale independently of cell density.

Conditional allele of *Dscam*

A conditional allele of *Dscam*, designated $Dscam^F$, was constructed by introducing loxP sites flanking the transmembrane encoding exon of *Dscam* by bacterial recombineering of the BAC BMQ238o15 (Copeland et al., 2001). The entire engineered BAC was linearized and electroporated into R1 ES cells. 200 ES cell colonies were screened by Southern blot analysis of EcoRI digested ES cell DNA. An EcoRI site was located upstream of the 5′ end of the BAC, and a probe between the EcoRI site and the beginning of the BAC was generated by PCR. Digestion with EcoRI resulted in an upshift of the band by 2 kb (12 to 14 kb), while double digestion with EcoRI and PmeI resulted in a decrease in size from 12 kb to 10 kb. 14 colonies with targeted integration were identified and three were injected into C57BL/6J blastocysts. Chimeric mice were bred to C57BL/6J and genotyped primers flanking the 5′ loxP site, which introduces 34 additional base pairs of DNA. The primers DscamCF (agc aaa agc acc atg att gac ag) and DscamCR (caa ctg act taa tga gtg gag) are used in PCR with the following conditions: 94° C denaturation for two minutes followed by 38 cycles of 94° C for twenty seconds, 60° C for thirty seconds and 72° C for 70 seconds, concluded with a final 4 minute incubation at 72° C.

Supplementary Material

Refer to Web version on PubMed Central for supplementary material.

Acknowledgments

We would like to thank Dr. Ignacio Provencio for generously providing the melanopsin antibody used in this study. We would also like to thank Drs. Vann Bennett (Duke University), Samar Hattar (John Hopkins University) and Lin Gan (University of Rochester) for generously providing mouse strains. We would also like to thank the Scientific Services at The Jackson Laboratory, particularly Light Microscopy and Histology and Cell Biology and Microinjection and the University of Idaho Optical Imaging Facility. We would also like to thank Dee Schramm, Andrew Garrett, Abby Tedenev and Holly Miller for help developing the project and editing the manuscript. This work was supported by grants from the National Institutes of Health (EY018605 to R.W.B. and EY020857 to P.G.F.), the Knights Templar Eye Research Foundation (P.G.F.). The Scientific Services at Jackson are supported by CA034196 and the University of Idaho Optical Imaging Facility is supported by P20RR016454.

References

Agarwala KL, Nakamura S, Tsutsumi Y, Yamakawa K. Down syndrome cell adhesion molecule DSCAM mediates homophilic intercellular adhesion. Brain Res Mol Brain Res. 2000; 79:118–126. [PubMed: 10925149]

Ahmed G, Shinmyo Y, Ohta K, Islam SM, Hossain M, Naser IB, Riyadh MA, Su Y, Zhang S, Tessier-Lavigne M, Tanaka H. Draxin Inhibits Axonal Outgrowth through the Netrin Receptor DCC. J Neurosci. 2011; 31:14018–14023. [PubMed: 21957262]

Andrews GL, Tanglao S, Farmer WT, Morin S, Brotman S, Berberoglu MA, Price H, Fernandez GC, Mastick GS, Charron F, Kidd T. Dscam guides embryonic axons by Netrin-dependent and -independent functions. Development (Cambridge, England). 2008; 135:3839–3848.

Barlow GM, Micales B, Chen XN, Lyons GE, Korenberg JR. Mammalian DSCAMs: roles in the development of the spinal cord, cortex, and cerebellum? Biochem Biophys Res Commun. 2002; 293:881–891. [PubMed: 12051741]

Blank M, Fuerst PG, Stevens B, Nouri N, Kirkby L, Warrier D, Barres BA, Feller MB, Huberman AD, Burgess RW, Garner CC. The Down syndrome critical region regulates retinogeniculate refinement. J Neurosci. 2011; 31:5764–5776. [PubMed: 21490218]

Buffelli M, Burgess RW, Feng G, Lobe CG, Lichtman JW, Sanes JR. Genetic evidence that relative synaptic efficacy biases the outcome of synaptic competition. Nature. 2003; 424:430–434. [PubMed: 12879071]

Campsall KD, Mazerolle CJ, De Repentingy Y, Kothary R, Wallace VA. Characterization of transgene expression and Cre recombinase activity in a panel of Thy-1 promoter-Cre transgenic mice. Dev Dyn. 2002; 224:135–143. [PubMed: 12112467]

Copeland NG, Jenkins NA, Court DL. Recombineering: a powerful new tool for mouse functional genomics. Nat Rev Genet. 2001; 2:769–779. [PubMed: 11584293]

Ecker JL, Dumitrescu ON, Wong KY, Alam NM, Chen SK, LeGates T, Renna JM, Prusky GT, Berson DM, Hattar S. Melanopsin-expressing retinal ganglion-cell photoreceptors: cellular diversity and role in pattern vision. Neuron. 2010; 67:49–60. [PubMed: 20624591]

Fuerst PG, Bruce F, Tian M, Wei W, Elstrott J, Feller MB, Erskine L, Singer JH, Burgess RW. DSCAM and DSCAML1 function in self-avoidance in multiple cell types in the developing mouse retina. Neuron. 2009; 64:484–497. [PubMed: 19945391]

Fuerst PG, Burgess RW. Adhesion molecules in establishing retinal circuitry. Curr Opin Neurobiol. 2009; 19:389–394. [PubMed: 19660931]

Fuerst PG, Harris BS, Johnson KR, Burgess RW. A novel null allele of mouse DSCAM survives to adulthood on an inbred C3H background with reduced phenotypic variability. Genesis. 2010; 48:578–584. [PubMed: 20715164]

Fuerst PG, Koizumi A, Masland RH, Burgess RW. Neurite arborization and mosaic spacing in the mouse retina require DSCAM. Nature. 2008; 451:470–474. [PubMed: 18216855]

Gan L, Xiang M, Zhou L, Wagner DS, Klein WH, Nathans J. POU domain factor Brn-3b is required for the development of a large set of retinal ganglion cells. Proc Natl Acad Sci U S A. 1996; 93:3920–3925. [PubMed: 8632990]

Gitton Y, Dahmane N, Baik S, Ruiz i Altaba A, Neidhardt L, Scholze M, Herrmann BG, Kahlem P, Benkahla A, Schrinner S, Yildirimman R, Herwig R, Lehrach H, Yaspo ML. A gene expression map of human chromosome 21 orthologues in the mouse. Nature. 2002; 420:586–590. [PubMed: 12466855]

Hattori D, Demir E, Kim HW, Viragh E, Zipursky SL, Dickson BJ. Dscam diversity is essential for neuronal wiring and self-recognition. Nature. 2007; 449:223–227. [PubMed: 17851526]

Hayashi S, McMahon AP. Efficient recombination in diverse tissues by a tamoxifen-inducible form of Cre: a tool for temporally regulated gene activation/inactivation in the mouse. Dev Biol. 2002; 244:305–318. [PubMed: 11944939]

Holtzman DM, Santucci D, Kilbridge J, Chua-Couzens J, Fontana DJ, Daniels SE, Johnson RM, Chen K, Sun Y, Carlson E, Alleva E, Epstein CJ, Mobley WC. Developmental abnormalities and age-related neurodegeneration in a mouse model of Down syndrome. Proc Natl Acad Sci U S A. 1996; 93:13333–13338. [PubMed: 8917591]

Hughes ME, Bortnick R, Tsubouchi A, Baumer P, Kondo M, Uemura T, Schmucker D. Homophilic Dscam interactions control complex dendrite morphogenesis. Neuron. 2007; 54:417–427. [PubMed: 17481395]

Kawaguchi Y, Cooper B, Gannon M, Ray M, MacDonald RJ, Wright CV. The role of the transcriptional regulator Ptf1a in converting intestinal to pancreatic progenitors. Nat Genet. 2002; 32:128–134. [PubMed: 12185368]

Keeley PW, Reese BE. Morphology of dopaminergic amacrine cells in the mouse retina: independence from homotypic interactions. J Comp Neurol. 2010; 518:1220–1231. [PubMed: 20148440]

Li HL, Huang BS, Vishwasrao H, Sutedja N, Chen W, Jin I, Hawkins RD, Bailey CH, Kandel ER. Dscam mediates remodeling of glutamate receptors in Aplysia during de novo and learning-related synapse formation. Neuron. 2009; 61:527–540. [PubMed: 19249274]

Liu G, Li W, Wang L, Kar A, Guan KL, Rao Y, Wu JY. DSCAM functions as a netrin receptor in commissural axon pathfinding. Proc Natl Acad Sci U S A. 2009; 106:2951–2956. [PubMed: 19196994]

Livet J, Weissman TA, Kang H, Draft RW, Lu J, Bennis RA, Sanes JR, Lichtman JW. Transgenic strategies for combinatorial expression of fluorescent proteins in the nervous system. Nature. 2007; 450:56–62. [PubMed: 17972876]

Ly A, Nikolaev A, Suresh G, Zheng Y, Tessier-Lavigne M, Stein E. DSCAM is a netrin receptor that collaborates with DCC in mediating turning responses to netrin-1. Cell. 2008; 133:1241–1254. [PubMed: 18585357]

Marquardt T, Ashery-Padan R, Andrejewski N, Scardigli R, Guillemot F, Gruss P. Pax6 is required for the multipotent state of retinal progenitor cells. Cell. 2001; 105:43–55. [PubMed: 11301001]

Masland RH. Neuronal diversity in the retina. Curr Opin Neurobiol. 2001; 11:431–436. [PubMed: 11502388]

Matsuoka RL, Nguyen-Ba-Charvet KT, Parray A, Badea TC, Chedotal A, Kolodkin AL. Transmembrane semaphorin signalling controls laminar stratification in the mammalian retina. Nature. 2011; 470:259–263. [PubMed: 21270798]

Matthews BJ, Kim ME, Flanagan JJ, Hattori D, Clemens JC, Zipursky SL, Grueber WB. Dendrite self-avoidance is controlled by Dscam. Cell. 2007; 129:593–604. [PubMed: 17482551]

Muzumdar MD, Tasic B, Miyamichi K, Li L, Luo L. A global double-fluorescent Cre reporter mouse. Genesis. 2007; 45:593–605. [PubMed: 17868096]

Nagy A, Gocza E, Diaz EM, Prideaux VR, Ivanyi E, Markkula M, Rossant J. Embryonic stem cells alone are able to support fetal development in the mouse. Development (Cambridge, England). 1990; 110:815–821.

Pecho-Vrieseling E, Sigrist M, Yoshida Y, Jessell TM, Arber S. Specificity of sensory-motor connections encoded by Sema3e-Plxnd1 recognition. Nature. 2009; 459:842–846. [PubMed: 19421194]

Rodieck RW. The density recovery profile: a method for the analysis of points in the plane applicable to retinal studies. Vis Neurosci. 1991; 6:95–111. [PubMed: 2049333]

Rowan S, Cepko CL. Genetic analysis of the homeodomain transcription factor Chx10 in the retina using a novel multifunctional BAC transgenic mouse reporter. Dev Biol. 2004; 271:388–402. [PubMed: 15223342]

Sanes JR, Zipursky SL. Design principles of insect and vertebrate visual systems. Neuron. 2010; 66:15–36. [PubMed: 20399726]

Savitt JM, Jang SS, Mu W, Dawson VL, Dawson TM. Bcl-x is required for proper development of the mouse substantia nigra. J Neurosci. 2005; 25:6721–6728. [PubMed: 16033881]

Schmucker D, Clemens JC, Shu H, Worby CA, Xiao J, Muda M, Dixon JE, Zipursky SL. Drosophila Dscam is an axon guidance receptor exhibiting extraordinary molecular diversity. Cell. 2000; 101:671–684. [PubMed: 10892653]

Soba P, Zhu S, Emoto K, Younger S, Yang SJ, Yu HH, Lee T, Jan LY, Jan YN. Drosophila sensory neurons require Dscam for dendritic self-avoidance and proper dendritic field organization. Neuron. 2007; 54:403–416. [PubMed: 17481394]

Stacy RC, Demas J, Burgess RW, Sanes JR, Wong RO. Disruption and recovery of patterned retinal activity in the absence of acetylcholine. J Neurosci. 2005; 25:9347–9357. [PubMed: 16221843]

Wang J, Zugates CT, Liang IH, Lee CH, Lee T. Drosophila Dscam is required for divergent segregation of sister branches and suppresses ectopic bifurcation of axons. Neuron. 2002; 33:559–571. [PubMed: 11856530]

Wassle H, Riemann HJ. The mosaic of nerve cells in the mammalian retina. Proc R Soc Lond B Biol Sci. 1978; 200:441–461. [PubMed: 26058]

Wojtowicz WM, Wu W, Andre I, Qian B, Baker D, Zipursky SL. A vast repertoire of dscam binding specificities arises from modular interactions of variable Ig domains. Cell. 2007; 130:1134–1145. [PubMed: 17889655]

Yamagata M, Sanes JR. Dscam and Sidekick proteins direct lamina-specific synaptic connections in vertebrate retina. Nature. 2008; 451:465–469. [PubMed: 18216854]

Yamagata M, Sanes JR. Synaptic localization and function of Sidekick recognition molecules require MAGI scaffolding proteins. J Neurosci. 2010; 30:3579–3588. [PubMed: 20219992]

Zhan XL, Clemens JC, Neves G, Hattori D, Flanagan JJ, Hummel T, Vasconcelos ML, Chess A, Zipursky SL. Analysis of Dscam diversity in regulating axon guidance in Drosophila mushroom bodies. Neuron. 2004; 43:673–686. [PubMed: 15339649]

Zhang DQ, Wong KY, Sollars PJ, Berson DM, Pickard GE, McMahon DG. Intraretinal signaling by ganglion cell photoreceptors to dopaminergic amacrine neurons. Proc Natl Acad Sci U S A. 2008; 105:14181–14186. [PubMed: 18779590]

Zhu H, Hummel T, Clemens JC, Berdnik D, Zipursky SL, Luo L. Dendritic patterning by Dscam and synaptic partner matching in the Drosophila antennal lobe. Nat Neurosci. 2006; 9:349–355. [PubMed: 16474389]

Highlights

- Conditional allele developed to test DSCAM cell autonomy
- DSCAM-mediated processes were genetically separated and are distinct
- *Dscam* regulates developmental cell death and spacing in a dose dependent manner
- DSCAM deficient cells induce a mutant phenotype on adjacent wild type cells of the same type
- DSCAM mediates arborization and spacing by acting within cell types and not between synaptically connected cell types

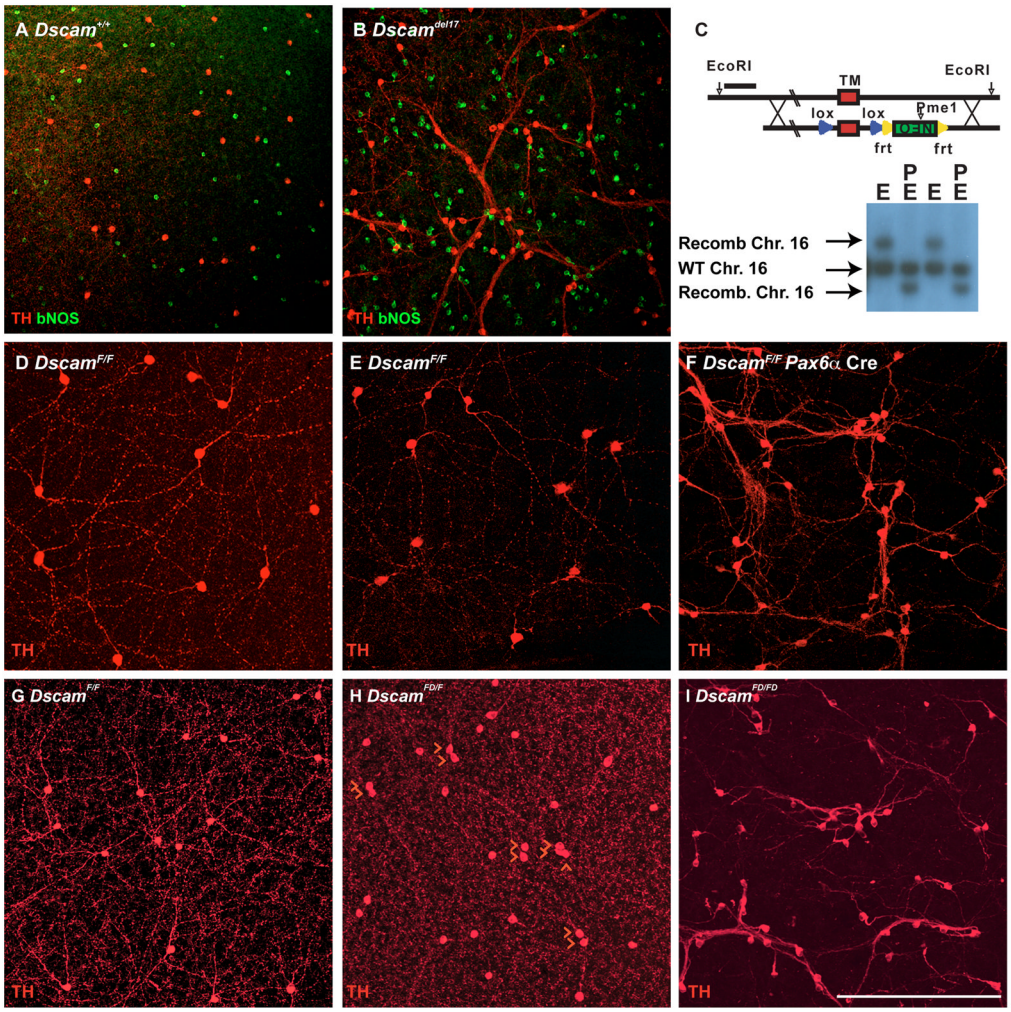

Figure 1. DSCAM-deficient phenotypes and *Dscam* conditional allele

A and **B**, Retinas stained with antibodies to tyrosine hydroxylase (TH) and brain nitric oxide synthetase (bNOS) to label dopaminergic (DA) and bNOS-positive amacrine cells, respectively. DA cell or bNOS cell neurites fasciculate with the neurites of other cells of the same type in $Dscam^{del17/del17}$ retinas but not across cell types. **C**, A conditional allele of *Dscam* was generated by flanking the exon encoding the *Dscam* transmembrane domain with loxP sites. An upstream EcoRI site was used for identifying homologous recombinants by Southern blotting. Recombination resulted in a 2 kb upshift when digested with EcoRI (E), or a 2 kb decrease in size if double digested with EcoRI (E) and PmeI (P), which cuts in the Neo-selectable marker. The results of Southern blotting DNA preps for two independent ES cell colonies are shown. The wild type Chromosome 16 (arrow) is cut by EcoRI resulting in a single band of approximately 12 kb. The recombined Chromosome 16 (arrow) is cut by EcoRI resulting in a single band of approximately 14 kb. The wild type Chromosome 16 (arrow) is cut by EcoRI and PmeI resulting in a single band of approximately 12 kb (PmeI has no cut sites within the EcoRI fragment). The recombined Chromosome 16 (arrow) is cut by EcoRI and PmeI resulting in a single band of approximately 10 kb (recombined sequence adds a PmeI site within the EcoRI fragment). **D**–**F**, $Dscam^{+/+}$, $Dscam^{F/F}$ and $Dscam^{F/F}$ *Pax6α* Cre retinas were collected at postnatal day 15 (P15) and stained with an antibody to TH. Cell bodies of wild type and $Dscam^{F/F}$ DA cells are spaced and have well arborized neurites, whereas conditional deletion of the *Dscam* transmembrane domain with *Pax6α* Cre

results in clumped DA cells and neurites. **G**–**I**, Germ line deletion of the conditional allele (*Dscam*^{FD}). Dopaminergic amacrine (DA) cells in retinas from P28 mice were stained with antibodies to TH. The number of DA cells directly adjacent to other DA cells was counted in each of four retinas and compared using a T-Test. *Dscam*$^{F/F}$ retinas had 10.5 +/− 1 DA cell pairs/retina while *Dscam*$^{FD/FD}$ retinas had 30.75 +/− 5.1 pairs/retina: T-Test=0.001. The scale bar in **I** is equivalent to 538.2 μm in **A** and **B**, 387.5 μm in **D**–**F** and 228 μm in **G**–**I**.

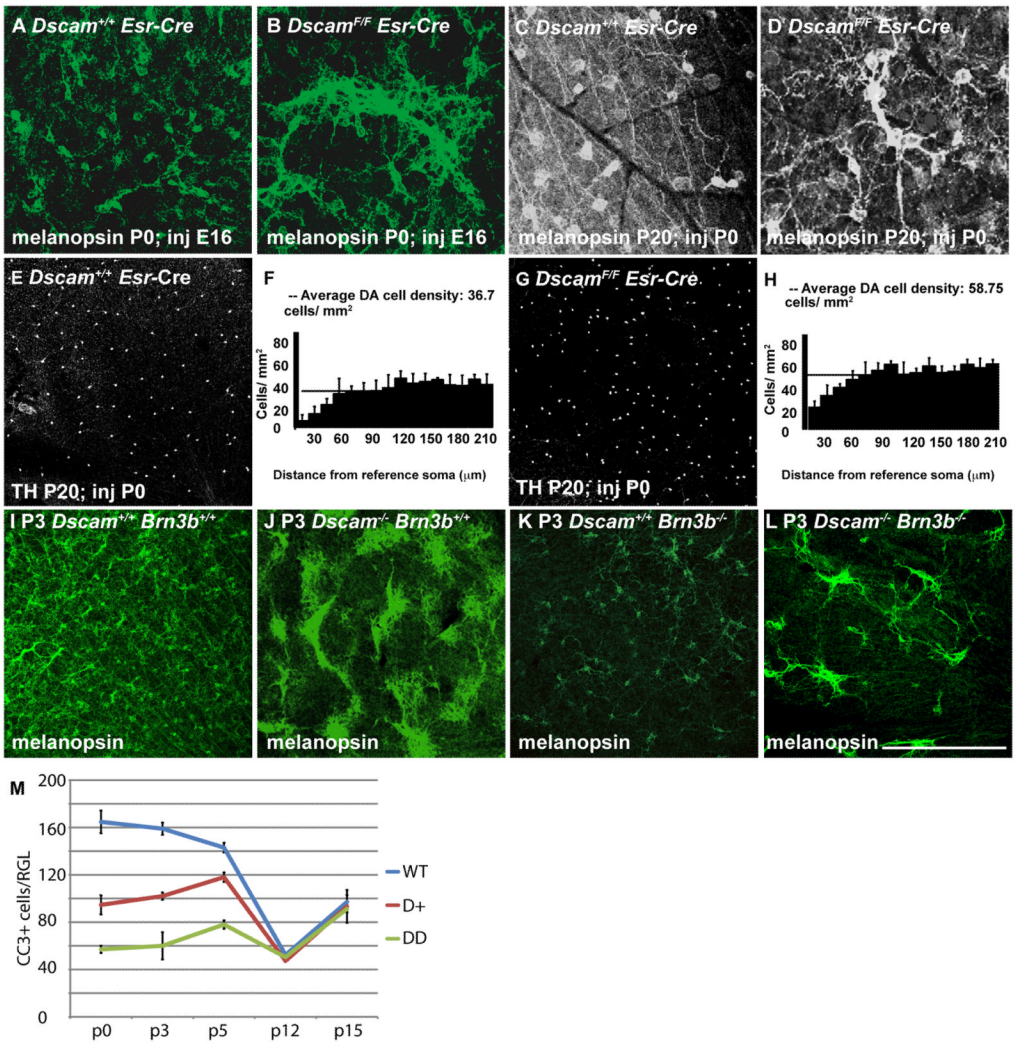

Figure 2. Independence of *Dscam*-dependent arborization and cell number regulation

A–**H**, The *Dscam* conditional allele was targeted using a tamoxifen-inducible Esr Cre. **A** and **B**, Retinas from P0 $Dscam^{+/+}$ Esr Cre and $Dscam^{F/F}$ Esr Cre mice, in which induction of Esr Cre was performed at embryonic day 16 (E16), were stained with antibodies to melanopsin. Widespread fasciculation and aggregation of mRGCs was observed in $Dscam^{F/F}$ Esr Cre retinas compared to $Dscam^{+/+}$ Esr Cre retinas (P0; N=4). **C**–**D**, Retinas from P20 $Dscam^{+/+}$ Esr Cre and $Dscam^{F/F}$ Esr Cre mice, in which induction of Esr Cre was performed at P0, stained with antibodies to melanopsin (N=3 and 5, respectively). $Dscam^{+/+}$ Esr Cre and the majority of $Dscam^{F/F}$ Esr Cre mRGCs had arborized dendrites and spaced soma. Occasional examples of fasciculation were observed in the $Dscam^{F/F}$ retinas. **E** and **G**, Retinas from P20 $Dscam^{+/+}$ Esr Cre and $Dscam^{F/F}$ Esr Cre mice, in which induction of Esr Cre was performed at P0, stained with antibodies to tyrosine hydroxylase (TH) (N=3). **F** and **H**, Density Recovery Profile (DRP) analysis was performed on DA cells from mice in which Esr Cre was induced at P0. The horizontal bar running across the vertical columns represents the average cell density. Vertical columns indicate the average number of cells located at a given distance from other cells of the same type, termed the reference soma. **F**, DA cells in retinas from $Dscam^{+/+}$ mice had an average cell density of 36.7 and had an exclusion zone, indicated by the lack of DA cells in close proximity to other DA cells, as represented by the vertical columns on the left hand side of the chart with reduced values

compared to the average cell density. **H**, DA cells in retinas from *Dscam*$^{F/F}$ mice had an average cell density of 60.4 and had an exclusion zone. **I**–**L**, Retinas from postnatal day 3 (P3) wild type, *Dscam*$^{del17/del17}$, *Brn3b*$^{-/-}$ and *Dscam*$^{del17/del17}$ *Brn3b*$^{-/-}$ mice were stained with antibodies to melanopsin, to label mRGCs. **I**, In the wild type retina mRGCs are distributed across the retina (N=4). **J**, In the Dscam$^{del17/del17}$ retina mRGC somata are densely clumped (N=4). **K**, The number of mRGCs is greatly reduced in the *Brn3b*$^{-/-}$ retina and have spaced soma (N=4). **L**, The number of mRGCs is reduced in the *Brn3b*$^{-/-}$;*Dscam*$^{del17/del17}$ retina. The remaining mRGCs present in the *Dscam*$^{del17/del17}$;*Brn3b*$^{-/-}$ retina are densely clumped (N=4). **M**, Whole retinas were stained with antibodies to cleaved caspase three (CC3) and the number of immuno-positive cells per retina was counted. A highly significant decrease in the number of cleaved caspase 3-postive neurons was observed when comparing *Dscam*$^{del17/del17}$, *Dscam*$^{del17/+}$ and *Dscam*$^{+/+}$ at postnatal days 0, 3 and 5 (T-Test < 0.002). No differences were detected at postnatal days 12 and 15 except between heterozygous and wild type at p12, which was comparatively small (T-Test=0.015). The scale bar in (**K**) is equivalent to 194 μm in **A** and **B**, 127.8 μm in **C** and **D,** 775 μm in **E** and **G** and 387.5 μm in **I**–**L**.

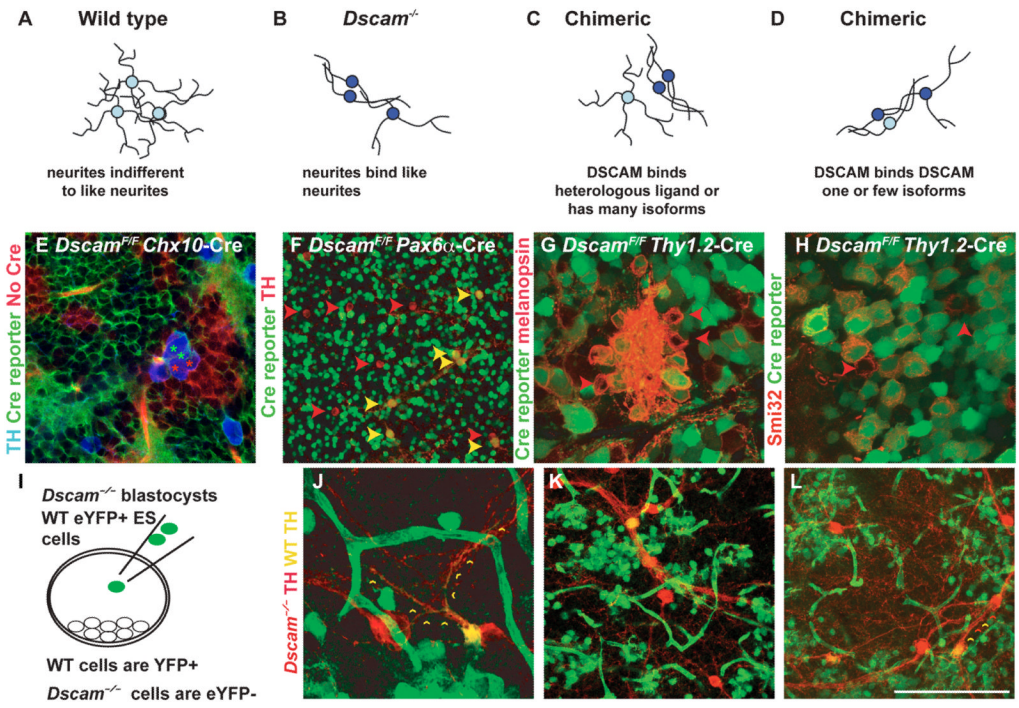

Figure 3. DSCAM-deficient cells induce mutant phenotype on wild type neighbors

Potential mechanisms of DSCAM-activity. **A**, In the wild type retina many neurons of a given type (homotypic neurons) arborize dendrites in an overlapping fashion. **B**, In the *Dscam*-deficient retina, homotypic-neurites fasciculate with each other. **C,** If DSCAM activity in the retina is mediated through interactions with a heterologous ligand, wild type cells will be expected to maintain a wild type phenotype in a chimeric retina. **D**, If DSCAM activity in the retina is mediated through homophilic interactions, wild type cells are predicted to clump and fasciculate with juxtaposed *Dscam* mutant cells, but not other wild type cells**. E**, *Chx10* Cre was used to delete *Dscam* from clonal columns of retina, Cre activity was monitored with a dual fluorescent Cre reporter such that dsRed (red) clonal columns lack Cre activity and eYFP (green) clonal columns indicate Cre activity (N>5). $Dscam^{FD/FD}$ (green asterisk) and wild type (red asterisk), or multiple $Dscam^{FD/FD}$ DA cells, were observed in aggregates as shown; however, multiple wild type DA cells were not observed to aggregate and fasciculate with each other. **F**, Image of central $Dscam^{F/F}$ Pax6α Cre retina stained with antibodies to TH. Variable expression of Cre results in a mix of wild type and mutant DA cells. Mutant DA cells were found localized next to either other mutant DA cells or wild type cells but wild type cells were rarely found juxtaposed next to other wild type DA cells, as in the wild type retina. **G** and **H**, *Dscam* was deleted from a subset of RGCs using Cre under control of the Thy1.2 promoter, indicated by a Thy1-floxed-stop-YFP Cre reporter (N>3). Aggregates of melanopsin positive (G) and SMI-32 positive alpha RGCs (H) contain a mixture of wild type (YFP-negative) and deleted neurons (YFP-positive). **I**, GFP-positive ES cells that are wild type for *Dscam* were injected into $Dscam^{del17/del17}$ blastocysts to generate chimeric retinas. Dopaminergic amacrine cells within chimeric retinas were labeled with an antibody to TH (N=2). **J**–**L**, Wild type dopaminergic amacrine cells (GFP-positive; yellow arrow head) aggregated and fasciculated with mutant dopaminergic amacrine cells (GFP-negative; red arrowhead). Small yellow arrowheads are placed along an example of cofasciculating wild type and mutant DA cell neurites. The scale bar in (**L**) is equivalent to 194 μm in **E** and **F**, 95 μm in **G**, 70 μm in **H**, 90 μm in **J** and 132 μm in **K** and **L**.

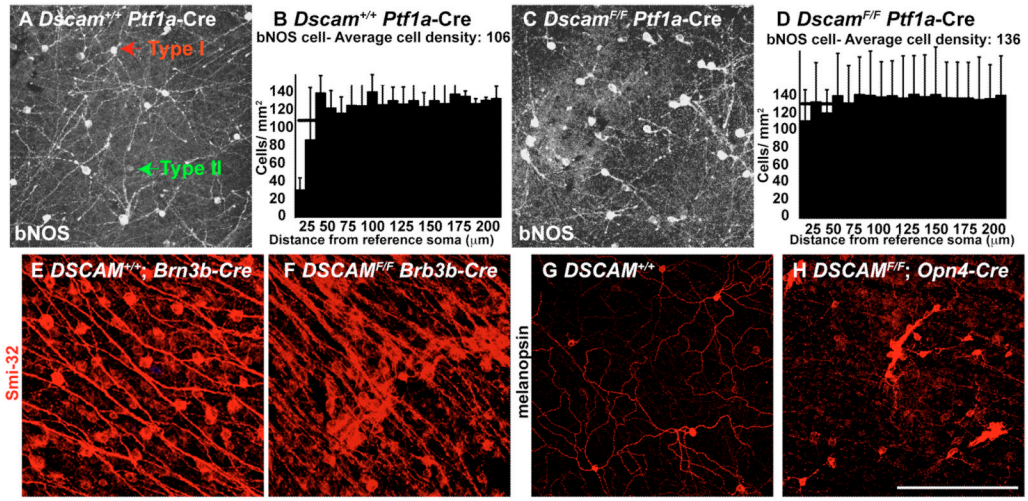

Figure 4. Cell type autonomous spacing defects after targeted deletion

Dscam was targeted using Cre lines active in either amacrine cells (*Ptf1a* Cre) or ganglion cells (*Brn3b* Cre and *Opn4* Cre). **A** and **C**, Retinas from P20 $Dscam^{+/+}$ *Ptf1a* Cre or $Dscam^{F/F}$ *Ptf1a* Cre mice were stained with antibodies to bNOS, to label bNOS-positive amacrine cells (N=3). Two types of amacrine cells are immunopositive for bNOS in the inner nuclear layer. Bright larger cells are type I bNOS-positive amacrine cells while smaller dimmer cells are type II bNOS-positive amacrine cells. Type I bNOS-positive amacrine cells (here fore referred to as bNOS amacrine cells) have fasciculated neurites in the $Dscam^{F/F}$ *Ptf1a* Cre retina (N=3). **B** and **D**, DRP analysis was performed on bNOS amacrine cells. **B**, bNOS amacrine cells from $Dscam^{+/+}$ *Ptf1a* Cre mice had an average cell density of 106 and a strong exclusion zone, as indicated by the vertical columns shorter than the average cell density on the left of the graph. **D**, bNOS amacrine cells from $Dscam^{F/F}$ *Ptf1a* Cre mice had an average cell density of 136 and lacked an exclusion zone, as indicated by the vertical columns roughly the same height as the average cell density on the left hand side of the graph. **E** and **F**, Retinas from P20 $Dscam^{+/+}$ *Brn3b* Cre and $Dscam^{F/F}$ *Brn3b* Cre mice were stained with antibodies to non-phosphorylated neurofilament (Smi-32). Smi-32 positive RGCs are aggregated and fasciculated in the $Dscam^{F/F}$ *Brn3b* Cre retina (**F**; N=3), while no spacing defect is observed in the $Dscam^{+/+}$ *Brn3b* Cre control retina (**E**; N=3). **G** and **H**, Retinas from P20 $Dscam^{+/+}$ *Opn4* Cre and $Dscam^{F/F}$ *Opn4* Cre mice were stained with antibodies to melanopsin, to label mRGCs. mRGCs are aggregated and fasciculated in the $Dscam^{F/F}$ *Opn4* Cre retina (**H)**, while no spacing defect is observed in the $Dscam^{+/+}$ *Opn4* Cre retina (**G**) (N=3). The scale bar in N is equivalent to 132 μm in **A** and **C**, 97 μm in **E** and **F** and 132 μm in **G** and **H**.

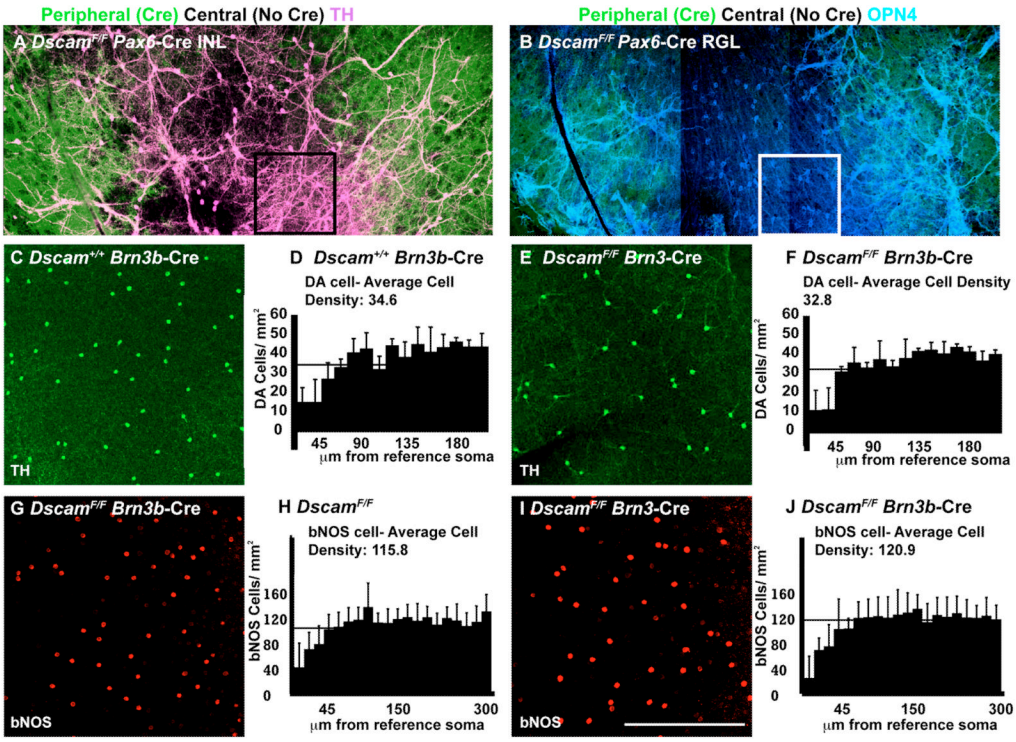

Figure 5. Lack of secondary spacing and arborization defects after *Dscam* deletion

Dscam$^{F/F}$ *Pax6α* Cre retinas stained with antibodies to TH and melanopsin to detect DA cells and mRGCs. **A**, Dopaminergic amacrine cells (DA) were imaged in the inner nuclear layer (INL) using an antibody to tyrosine hydroxylase (TH). DA cells were clumped and had fasciculated dendrites throughout the retina. **B**, In the same retina, melanopsin-positive RGCs (mRGCs) were imaged in the retinal ganglion layer (RGL) using an antibody to melanopsin. mRGCs were clumped and had fasciculated dendrites in the peripheral RGL, where Cre was active in the RGL, but not in the central and dorsal retina, where Cre activity was absent in the RGL. **A** and **B**; inset, Sample area of retina in which DA cells are clumped and have fasciculated neurites in the INL (**A**), but mRGCs are spaced and have arborized dendrites (**B**). **C**–**F**, Spacing and arborization of dopaminergic amacrine cells was assayed in *Dscam*$^{+/+}$ *Brn3b* Cre and *Dscam*$^{F/F}$ *Brn3b* Cre retinas. DA cells were labeled with an antibody to TH. **C** and **E**, Dopaminergic amacrine cells have spaced soma and arborized neurites in *Dscam*$^{+/+}$ *Brn3b* Cre and *Dscam*$^{F/F}$ *Brn3b* Cre retinas (N=3). DRP analysis was performed on DA cells from *Dscam*$^{+/+}$ *Brn3b* Cre and *Dscam*$^{F/F}$ *Brn3b* Cre retinas. **D**, DA cells in the retinas of *Dscam*$^{+/+}$ *Brn3b* Cre mice had an average cell density of 34.6 and a strong exclusion zone, as indicated by the vertical columns shorter than the average cell density on the left of the graph. **F**, DA cells from *Dscam*$^{F/F}$ *TH* Cre mice had an average cell density of 32.8 and a strong exclusion zone, as indicated by the vertical columns shorter than the average cell density on the left of the graph. **G**–**J**, Spacing and arborization of bNOS-positive amacrine cells were assayed in *Dscam*$^{F/F}$ and *Dscam*$^{F/F}$ *Brn3b* Cre retinas (N=5). bNOS amacrine cells were labeled with an antibody to bNOS. **G** and **I**, bNOS-positive amacrine cells have spaced soma and arborized neurites in retinas from *Dscam*$^{F/F}$ and *Dscam*$^{F/F}$ *Brn3b* Cre retina mice. **H** and **J**, DRP analysis was performed on bNOS cells from *Dscam*$^{F/F}$ and *Dscam*$^{F/F}$ *Brn3b* Cre retinas. **H**, bNOS cells in the retinas of *Dscam*$^{F/F}$ mice had an average cell density of 115.8 and a strong exclusion zone, as indicated by the vertical columns shorter than the average cell density on the left of the graph. **J**, bNOS cells from *Dscam*$^{F/F}$ *Brn3b* Cre mice had an average cell density of 120.9 and had an exclusion

zone, as indicated by the vertical columns shorter than the average cell density on the left of the graph. The scale bar in (**I**) is equivalent to 440 μm in **A** and **B** and 387.5 μm in **C**, **E** and 317.5 μm in **G** and **I**.

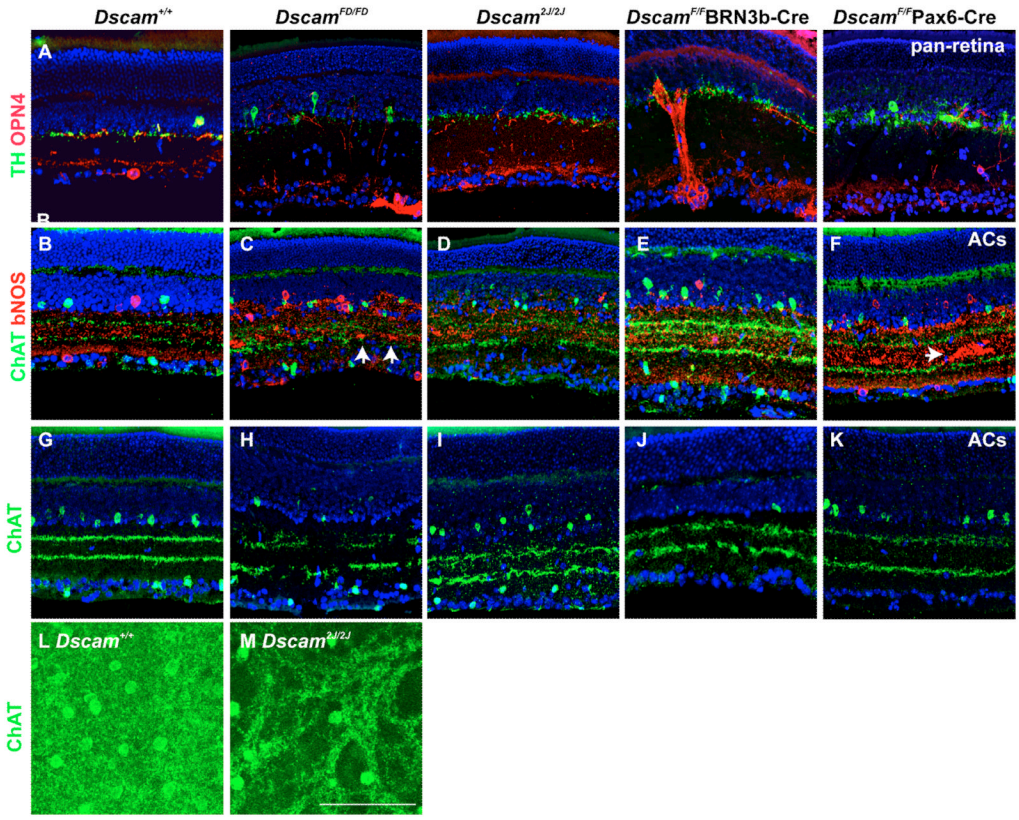

Figure 6. Dscam lamination phenotypes

Sections of retina from *Dscam*$^{FD/FD}$, *Dscam*$^{2J/2J}$ mice and *Dscam*$^{F/F}$ mice targeted with Pax6α Cre or Brn3b Cre were stained with antibodies to TH, OPN4, Syt2 and ChAT. **A**, DA cells normally laminate processes along the inner nuclear layer. mRGCs normally laminate adjacent to the inner nuclear layer and slightly offset proximal to the retinal ganglion cell layer. DA cells and mRGCs maintain normal lamination patterns in wild type and *Dscam* mutant retinas. **B**–**K**, Retinas from wild type, *Dscam*$^{FD/FD}$, *Dscam*$^{2J/2J}$ and *Dscam*$^{F/F}$ Pax6α Cre and Brn3b Cre mice were stained with antibodies to choline acetyl transferase (ChAT) to label cholinergic amacrine cells (B–K) and bNOS to label bNOS positive amacrine cells (B–F). **B**, bNOS labels three bands of neurites in the wild type inner plexiform layer. **C** and **D**, This pattern of lamination is lost in the *Dscam*$^{FD/FD}$ and *Dscam*$^{2J/2J}$ retina. **E** and **F**, bNOS lamination is maintained in the *Dscam*$^{F/F}$ Brn3b Cre retina and in portions of the *Dscam*$^{F/F}$ Pax6 Cre retina in which amacrine cells only are targeted, despite the presence of fasciculation (arrow). **B** and **G**, The neurites of cholinergic amacrine cells laminate in two bands in the wild type retina. **C**, **D**, **H** and **I**, Breaks in the lamination of cholinergic amacrine cell neurite bands are present in the *Dscam*$^{FD/FD}$ and *Dscam*$^{2J/2J}$ retina. **E** and **J**, Cholinergic amacrine neurite bands are disrupted in the *Dscam*$^{F/F}$ Brn3b Cre retina, although not to the degree observed *Dscam*^{FD} or *Dscam*^{2J} mice. **F** and **K**, Cholinergic amacrine cell neurite bands laminate evenly in regions of the *Dscam*$^{F/F}$ Pax6α Cre retina in which Cre is only expressed in amacrine cells. **L** and **M**, Whole wild type and *Dscam*$^{2J/2J}$ retinas were stained with antibodies to ChAT to label cholinergic amacrine cells. The inner nuclear layer and OFF cholinergic band was imaged. Cholinergic amacrine cells arborize a diffuse net of processes in the wild type retina but this pattern is disrupted in the *Dscam*$^{2J/2J}$ retina. The scale bar in (**K**) is equivalent to 105 μm in **A**–**K** and 52 μm in **L** and **M.**

Dev Biol. Author manuscript; available in PMC 2013 January 15.

Table 1

Phenotypes associated with *Dscam* alleles and conditional deletion

Genotype	Target cell type	Fasciculation	Cell Number	Spacing	Notes
$Dscam^{Del17/Del17}$	Pan-Retina	++++	++++	++++	First published *Dscam* mutant
$Dscam^{F/F}$	Pan-Retina	++++	++++	++++	Largely recapitulates frame shift alleles
$Dscam^{F/F}$ Brn3b-Cre	Most RGCs	++++	++++ or N.D.**	++++	Minimal cofasciculation of DA and mRGCs
$Dscam^{F/F}$ Opn4-Cre	mRGCs	++++	++++	++++	Opn4 Cre targets many types of RGCs; Minimal cofasciculation of DA and mRGCs
$Dscam^{F/F}$ Thy1-Cre	Many RGCs and amacrine cells	++++	++++	++++	non-autonomous spacing defects in DA cells
$Dscam^{F/F}$ Chx10-Cre	All or none in clonal columns	++++	++++	++++	Demonstrates requirement for homophilic signaling.
$Dscam^{F/F}$ Pax6-Cre	All	++++	++++	++++	Peripheral/Ventral portion of retina
$Dscam^{F/F}$ Pax6 Cre	Most amacrine cells	++++	N.D.	++++	Central/Dorsal portion of retina
$Dscam^{F/F}$ TH Cre (Jax #008601)	DA cells	−	++ (variable)	++ (variable)	Some mice had wild type phenotype
$Dscam^{F/F}$ Ptf1A Cre	GABAergic amacrine cells	++	−	++	
$Dscam^{F/F}$ SHH Cre	RGCs	+ (D.N.S.)	+ (D.N.S)	+ (D.N.S.)	
$Dscam^{F/F}$ ChAT Cre	Cholinergic amacrine cells	N.A.	− N.O.	N.A.	Cholinergic lamination phenotype not observed after targeting with Chat- Cre
$Dscam^{F/F}$ TH-Cre B6.FVB(Cg)-Tg(Th-cre)FI172Gsat/Mmcd	DA cells	−	−	−	No Cre activity detected in DA cells
$Dscam^{F/F}$ Esr-Cre E12 induction	Pan-Retina	++++	++++	++++	Largely recapitulates frame shift alleles
$Dscam^{F/F}$ Esr-Cre P0 induction	Pan-Retina	− DA + mRGC	++ DA N.O. mRGC	++	
$Dscam^{F/F}$ Esr-Cre P5 or older induction	Pan-Retina	D.N.S.	N.O.	N.O.	Demonstrates early period of Dscam function

N.A. Not Applicable

N.D. Not Determined

N.O. Not Observed but not quantified

D.N.S. Data Not Shown